High-Energy Solid-State Lithium Batteries with Organic Cathode Materials

Award No: EE0008234

Final Report

Submitted to
Tien Q Duong
Office of Vehicle Technologies
Energy Efficiency and Renewable Energy
U.S. Department of Energy

Submitted by
Yan Yao
Principal Investigator
Department of Electrical and Computer Engineering
University of Houston
Phone: 713-743-4432
yyao4@uh.edu

Team Member
Jun Lou
Co-Principal Investigator
Department of NanoEngineering
Rice University
Phone: 713-348-3573
jlou@rice.edu

Abstract

Organic materials made from abundant elements via low-energy processes are emerging as sustainable and low-cost alternatives to transition metal oxides as the electrode materials for high-energy batteries in the wake of supply chain and environmental issues associated with critical materials during the transition to clean energy. Organic insertion materials (OIMs) offer material-level energy comparable to transition metal oxides, but they have durability difficulties owing to dissolving in common liquid electrolytes. Combining ceramic-based solid electrolytes with organic electrode materials is one intriguing solution. The goal of this project is to design and synthesize high-energy OIMs, to understand the chemical dynamics and mechanical properties at the OIM-sulfide interface during electrochemical cycling, and to develop methods for constructing the optimum cathode microstructure, which will lead to improved electrochemical performance. The project team has accomplished the following over the last four years: (a) demonstrating that the mechanical softness of organic electrode materials is uniquely beneficial in suppressing crack formation at the electrode-electrolyte interface during cell operation; (b) understanding the interaction between cathode microstructure and the mechanical properties of individual components; and (c) establishing predictive control of cathode microstructure by tuning the mechanical properties of solid electrolytes and OIMs; (d) determining the chemical combability of sulfide electrolyte with high-energy OIMs and finally (f) laying out a road map toward a specific energy of 500 Wh kg^{-1} for solid-state lithium batteries. 14 publications resulted from this project.

PROJECT OBJECTIVE: The objective of this project is to research, develop, and demonstrate a multi-electron organic insertion material (OIM) for solid-state Li batteries capable of achieving an energy density ≥500 Wh/Kg while achieving a ≥500 cycle life.

PROJECT IMPACT: Electrode materials such as OIMs and sulfur are increasingly popular for high-energy solid-state batteries, but they only show desirable material utilization at a low active ratio. Based on our studies on OIMs and comparison with sulfur batteries, we have identified that the property of the active materials relative to that solid electrolytes as the origin of the problem. The common practice to tackle low utilization has been nanoscale mixing. While successful to some extent, this strategy alone does not address the fundamental property mismatch issue and hence fails to increase active ratio to practical levels. We have demonstrated solutions to attack the problem and used suitable tools to validate our approaches. The technology developed in this work will enable high-energy cells based not only on OIMs but any electrode materials that share the same characteristics such as sulfur cathodes.

APPROACH: We use high-energy OIMs to systematically address the general property-mismatch dilemma faced by organic cathode materials, thereby ensuring the high specific energy demonstrated from the active material level is maintained at the cell level. The project will be divided into two parts: first, we will explore strategies to achieve a favorable microstructure of the OIM–electrolyte composites; second, OIMs with higher specific energy than that achieved in Phase 1 will be developed. We expect more advanced OIMs, along with optimized microstructure, to achieve Battery500 targets.

OUT-YEAR GOALS: Demonstrate solid-state OIM–Li batteries with optimized electrode microstructures. This is achieved by using our benchmark OIM to establish methods for OIM property tuning via chemical lithiation and electrolyte coating. In addition, nanoscale mixing of OIMs with solid electrolytes will be systematically investigated. By the end of the project, we expect the active material ratio in the cathode to significantly increase without impacting material utilization and energy efficiency.

COLLABORATIONS: This project collaborates with Prof. Ardebili at the University of Houston, Prof. Kejie Zhao at Purdue University on mechanical property measurement of solid electrolytes.

During Phase 1 of the project, we introduced a class of high-energy cathode materials, organic insertion materials (OIMs), to pursue the 500-Wh/kg specific energy target set by the Battery500 Consortium. These materials complement the high nickel manganese cobalt (NMC) and sulfur that are under active development within the Battery 500 Consortium. At the active material level, OIM–Li, NMC–Li, and sulfur–Li all deliver specific energy values of ~1000 Wh/kg (Fig. 1a), which may translate into ~500 Wh/kg at the cell level. Both the working potential and specific capacity of typical OIMs sit between those of NMC and sulfur, rendering OIMs two unique features: (1) better compatibility than NMC with solid electrolytes that have limited anodic stability such as sulfide superionic conductors; (2) no drastic volume change like sulfur. While the cycle life of high-energy OIMs had been limited in liquid-state lithium batteries, we proposed to address the issue with all-solid-state cell designs. OIMs are softer than ceramic cathode materials and even sulfide electrolytes (Fig. 1b), which property makes them particularly suitable for constructing solid-state cells.

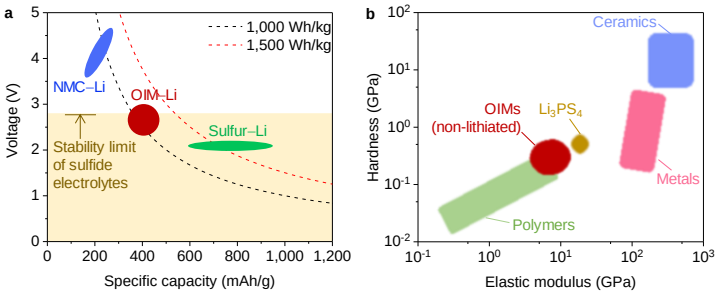

Figure 1. Characteristics of OIMs. a, Specific energy of OIM–Li compared with those of other batteries under investigation within the Battery500 consortium. The potential of cathode materials relative to the anodic stability potential of solid-state sulfide electrolytes is also shown. b, Mechanical properties of materials relevant to solid-state batteries.

In Phase 2, we explore approaches to significantly increase the active material ratio and translate high material-level specific energy to the cell level. In addition, new OIMs with higher specific capacity and potential has been developed. We have established baseline spectroscopic methods for characterization of the microstructures of composite cathodes in solid-state batteries. Quantitative structural analysis was conducted on composite cathodes by FIB-SEM tomography. The cross-section of a composite cathode was polished using FIB, and then imaged with SEM. This ion-slice (50-nm thick), electron-image sequence was repeated until a sufficient thickness of the sample has been serial imaged. The 3D tomogram was then reconstructed by vertical stacking of the aligned 2D SEM images. Fig. 2 shows the result of a 4-micron-cube block. Three phases of main interest are identified in Fig. 2a: solid electrolytes which appear light, active materials which appear gray, and voids which appear dark. The distribution of them can be seen in Fig. 2b-d, respectively. For this specific electrode, the volume fraction of the solid electrolyte, active material, and voids is 65%, 22%, and 13%, respectively.

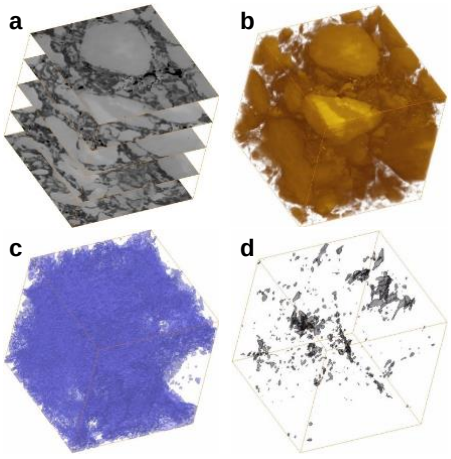

Figure 2. FIB-SEM tomography of a solid-state composite cathode. A, Selected slides of SEM images. B–D, 3-D rendering of solid electrolyte (B), cathode active material (C), and voids (D).

Our baseline cell was based on an OIM cathode: OIM particles, sulfide electrolytes and conductive carbon are mechanically milled as dry powders, and the resulted mixture is then cold-pressed into a pellet. This procedure is thereafter referred to as dry-mixing (Fig. 3a). A specific capacity of 407 mAh/g is achieved when the OIM ratio of 20 wt%, but this performance is not sustained at higher active material ratios, such as 30 wt%. Our preliminary studies indicated that the performance drop originated from the formation of unfavorable microstructures of the composite electrode, which has decreased ionic conduction within the cathode. We expect restoration of efficient ionic conduction as long as a good network of solid electrolyte is retained despite a change in the active material–solid electrolyte ratio. We have explored methods to improve the microstructures. One of the most effective ways that we have identified so far is wet mixing (Fig. 3b). Solid electrolytes were dissolved into a solution, to which OIM particles were added, stirred, and ground. Upon complete removal of the solvent in the electrolyte solution via evaporation followed by thermal annealing, the solid electrolyte precipitated onto OIM particles, effectively forming a uniform ion-conductive coating. The OIM–solid electrolyte composite was then ground with conductive carbon and cold-pressed into a pellet, similar to what was done in a dry-mixing procedure.

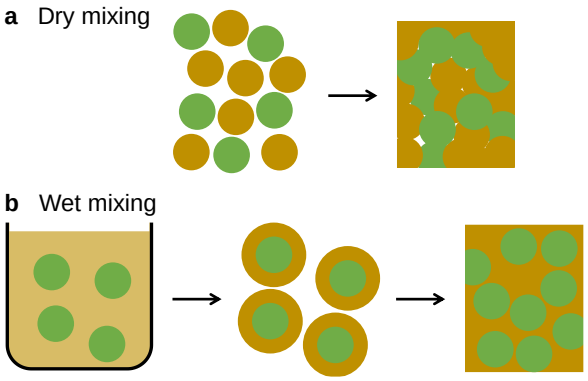

Figure 3. Electrode fabrication methods for OIM-based cathodes. a, Dry-mixing involving OIM powders (green), sulfide electrolyte powders (brown), and conductive carbon (omitted). b, Wet-mixing involving coating OIM particles with sulfide electrolyte using a wet-mixing method.

The effectiveness of the wet-mixing procedure was examined with imaging techniques at different levels. Fig. 4a and b compare the morphology of OIM–solid electrolyte composite powders prepared via dry- and wet-mixing. The dry-mixed powers (Fig. 4a), prepared by mechanically milling dry powders of the OIM and the solid electrolyte, show large agglomerates and apparent phase segregation as told by the distinct morphological features in different areas of

the image. The wet-mixed powders (Fig. 4b), prepared by first preparing a solution of the solid electrolyte in an inert solvent and then mixing it with the OIM powders and drying, show much finer particles and a more uniform feature distribution. Observation of the cross-section of the electrodes fabricated by cold-pressing the two composite powders revealed a largely broken solid-electrolyte network with the dry-mixed powders (Fig. 4c) as opposed to a much more connected one with the wet-mixed ones (Fig. 4d). The electrode made from wet-mixed powders is thus expected to be more likely to achieve high performance.

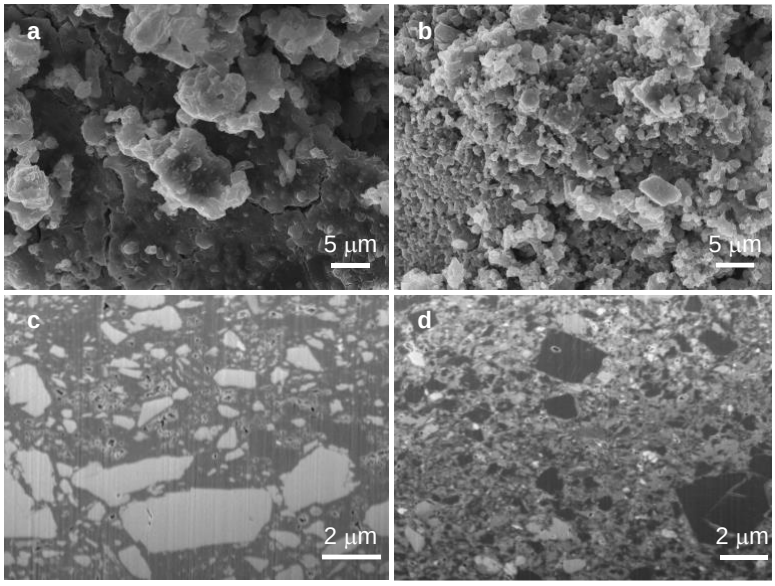

Figure 4. SEM observation of the morphology of OIM–solid electrolyte composite powders and electrodes. Powders (a and b) and cross-sections of electrodes (c and d) made from dry- (a and c) and wet-mixing (b and d) of OIM and solid electrolyte.

We have also resorted to chemical tools to distinct the two electrodes. One such tool is secondary ion mass spectrometry with time-of-flight mass analysis (ToF-SIMS). It provides quantitative chemical information on even trace species with high spatial resolution. Fig. 5 shows the three-dimensional profiling of Li^+ in the two electrodes. Since the OIM examined has no Li in its formula, the only species in the composite electrode that has Li^+ is the solid electrolyte. The Li^+ profile thus indicate the spatial distribution of the solid electrolyte. Fig. 5a shows the solid electrolyte forms large aggregates, and a considerable portion of the electrode has limited access to the electrolyte network. The size of the aggregates agrees with the SEM observation of the powders. The electrode made of wet-mixed powders shows much more uniform solid electrolyte distribution (Fig. 5b), with all regions fully penetrated by the solid electrolyte network, at least at the scale of observation. Wet mixing is thus a more effective way to fabricate a solid-state cathode. More quantitative analyses based off the characterization tools involved herein will be performed in the future to give further insights into the structural characteristics and optimization strategies of the wet-mixed electrodes.

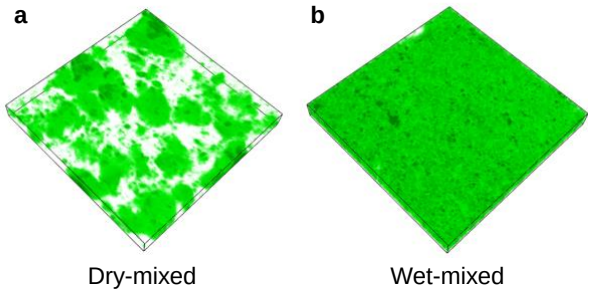

Figure 5. ToF-SIMS observation of the Li^+ distribution in OIM–solid electrolyte composite cathodes. a, Electrode made from dry-mixed powders shown in Figure 1a. b, Electrode made from wet-mixed powders. Horizontal scale: 60 × 60 μm^2. Vertical scale: not determined.

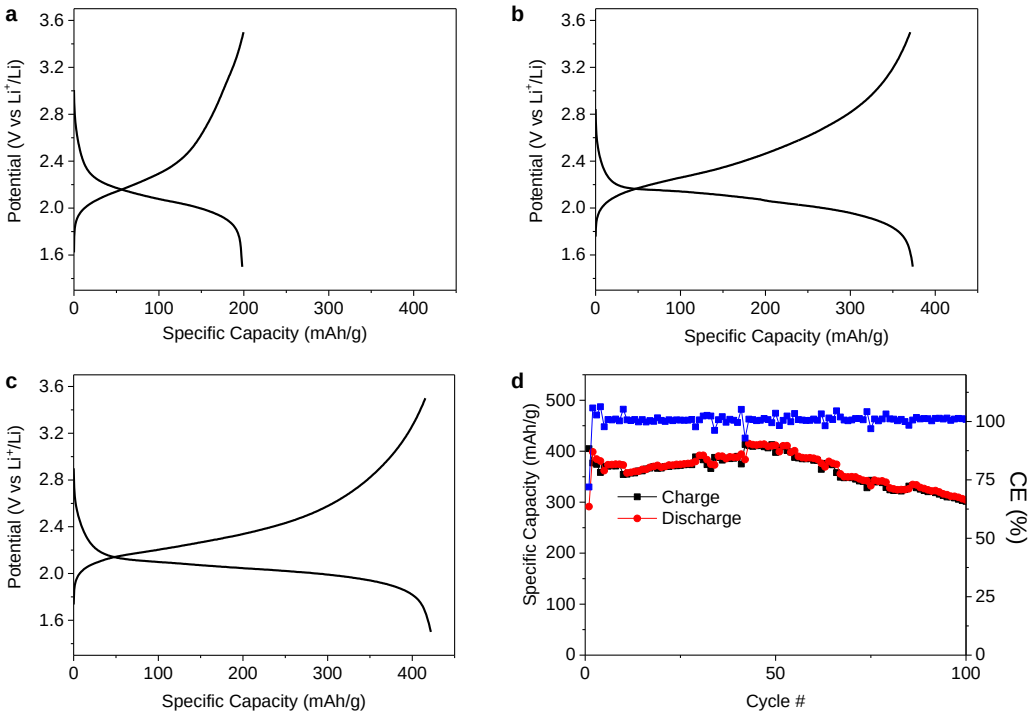

Figure 6. Voltage profiles (a–c) and cycling stability (d) of OIM–solid electrolyte composite cathodes with an active material ratio of 40 wt.%. a, Electrode made from dry-mixed powders, as shown in Figure 3a. b, Electrode made from wet-mixed powders, as shown in Figure 3b. c and d, Electrode made from wet-mixed powders, with the particle size of the OIM powders further reduced.

The electrochemical performance of the electrodes made from different processing methods have been evaluated and compared. At the relatively high active material ratio of 40 wt.%, the electrode made via simple dry mechanical milling delivered a specific capacity of ~200 mAh/g (Fig. 6a), which is only half of that achieved at an active ratio of 20 wt.% (baseline cell). The electrode made from wet-mixed powders shows massively improved (+85%) specific capacity (Fig. 6b), which may be attributed to the much improved ionically conducting network. Now that the solid electrolyte is evenly distributed throughout the electrode, the domain of the OIM itself becomes the limiting factor to the electrode uniformity. We tentatively attend to this issue by reducing the particle size of the OIM by downsizing the OIM powders via mechanical milling before subjecting them to the solution processing. The result is further improved specific capacity (Fig. 6c), now matching that obtained with electrodes containing 20 wt.% of active OIMs. The electrode showed a capacity retention of 76% after 100 cycles (Figure 6d).

The origin of the active material-in-electrolyte structure of solution-processed LPSCl–PTO is investigated in greater depth. Nanoindentation measurements in SEM reveals the regional mechanical property of a finely mixed composite. A detailed probe of pristine PTO, LPSCl, and the composites of the two processed with different methods was thus performed (Fig. 7). The Young's modulus of pritine LPSCl (39.2 ± 14.0 GPa) is five times as high as that of pristine PTO (6.0 ± 1.3 GPa). Upon dry-processing, the modulus of LPSCl is largely unchanged (43.8 ± 6.8

GPa), while that of PTO increases by two times to 18.9 ± 3.9 GPa. We attribute the increase to the reduction of PTO by LPSCl, which leads to partial lithiation of the molecular material and renders the solid partly ionic. It is well known that organic compounds held by ionic bonds have higher moduli than those held by van de Waal forces. The increase of PTO's modulus in the dry-processed composite, however, is not great enough to reverse the electrolyte-in-active material microstructure. In solution-processing, the reaction between PTO and LPSCl is facilitated due to the increased reaction area and improved mass transport in the liquid phase, and the lithiation of PTO proceeds to a greater extent. The modulus of PTO increases to 29.9 ± 4.4 GPa as the result. This increase alone still would not have been enough to reverse the microstructure. The simultaneous decrease in modulus of LPSCl (21.9 ± 4.2 GPa) in this process plays a critical role. Now that the hardened PTO is harder than the softened LPSCl, a reversed structure can be formed.

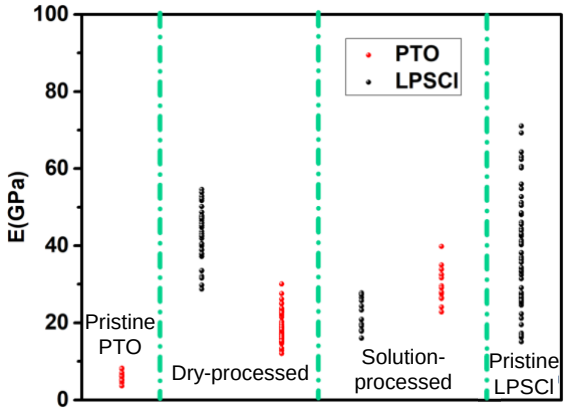

Figure 7. Young's moduli of pristine, dry-processed, and solution-processed PTO and LPSCl.

The softening of LPSCl and its potential impact on cell performance was examined. A control LPSCl sample solution-processed without added PTO was dried from the solvent and subjected to thermogravimetric analysis. A 20% weight loss was observed around 100 °C, with minor weight loss to follow through up to 600 °C (Fig. 8a). The analysis suggests an appreciable amount of solvent is trapped within the solid electrolyte, likely in both physisorption (related to solvent released at lower temperatures) and chemisorption forms (those lost at higher temperatures). Such formation was detected by X-ray diffraction. After solution-processing but before any dedicated heat treatment, the XRD pattern of LPSCl is complete different from a pristine sample (Fig. 8b), an indication of solvation as previously reported in solvent treatment of

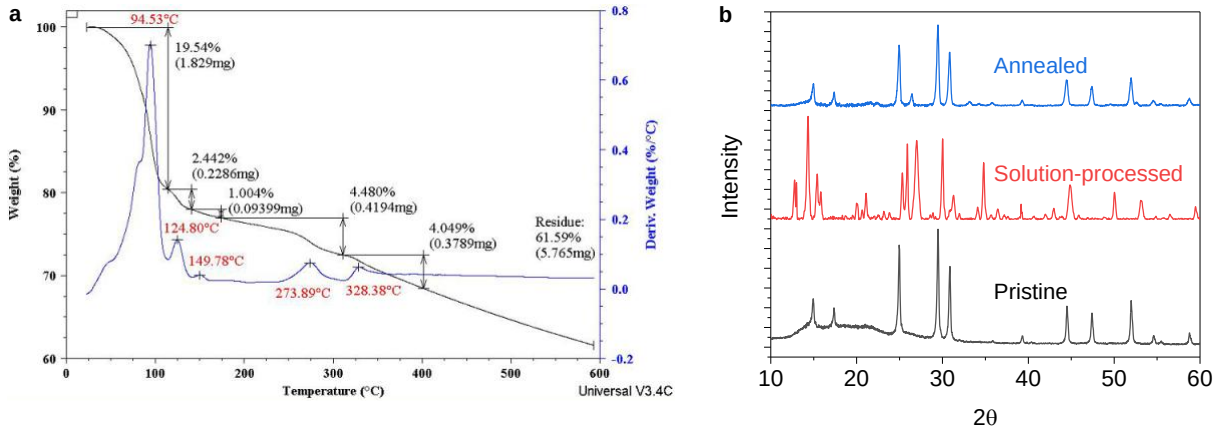

Figure 8. Characterization of processed LPSCl. a, Thermogravimetric analysis of solution-processed LPSCl. b, Comparison of pristine, solution-processed, and annealed LPSCl.

sulfide electrolyte. Annealing at 550 °C transform the electrolyte almost completely to the original state, with only peaks related to minor impurities remain. This reversible transformation of sulfide electrolytes can be utilized as a way to temporarily modify their mechanical property for electrode fabrication. The solution-processed sulfides are softened precursors that allow formation of unique microstuctures otherwise impossible, such as the active material-in-electrolyte structure of solution-processed LPSCl–PTO. Once the desired microstructure is formed, any solvent introduced can be removed by heat treatment, and the crystalinity and conductivity of the electolyte are recovered.

Solution-processed sulfide electrolytes show decreased Young's moduli and hardness compared with their pristine forme. The change provides flexibility to engineer cathode composite microstructure and new dimensions for tuning cell performance. As part of the continued effort to incorporate higher-capacity and higher-voltage organic cathode materials into solid-state cell using the solution-processing method, we have looked deeper into the property changes of solution-processed electrolytes and how to control them during cell fabrication. The weight loss of solution-processed electrolyte at elevated temperatures was studied with thermal gravimetric analysis-mass

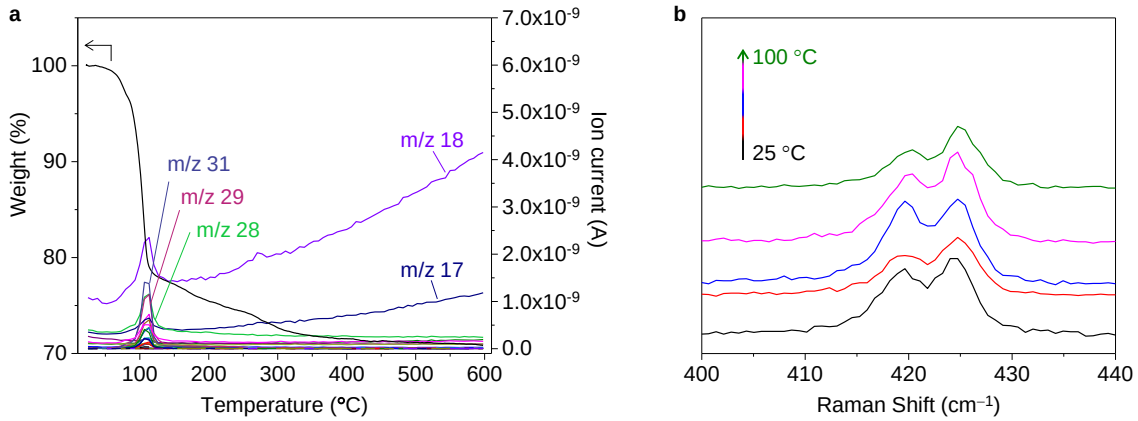

Figure 9. Probing the temperature-dependent evolution of the solvent-processed electrolyte. a, Thermal gravimetric analysis-mass spectroscopy characterization of the electrolyte as-processed. b, Raman spectra of the processed electrolyte heat-treated at increasing temperatures.

spectroscopy (Fig. 9a). The major weight loss between 60 and 110 °C coincides with the emergence of fragments at *m*/*z* 28 ($C_2H_4^+$), 29 ($C_2H_5^+$), and 31 (CH_3O^+), indicating removal of organic solvents. The weight loss afterwards mainly associates with *m*/*z* 17 (OH^+) and 18 (H_2O^+), which is attributable to moisture introduced during sample transfer and not the electrolyte. The property change before the stabilization of the chemical composition of the electrolyte (i.e., before 110 °C) is therefore of particular interest. Raman spectra of the solution-processed electrolyte heat-treated at increasing temperatures reveals a gradual increase of the peak intensity at 425 cm^{-1} relative to that at 419 cm^{-1} as the temperature increases from 25 to 100 °C (Fig. 9b).

The thermal evolution of the solution-processed solid electrolyte indicates the importance to consider the thermal history of components during cathode preparation. A preliminary demonstration of the effect of thermal history on cell performance has been carried out with

cathodes prepared with judiciously modified annealing procedures (Fig. 10a). Our previous procedure for cathode preparation includes solution-assisted mixing of the active material, electrolyte, and conductive agent, annealing the composite, and compressing the composite into compact layer for cell fabrication. This procedure effectively utilizes the properties of the electrolyte observed at higher temperatures.

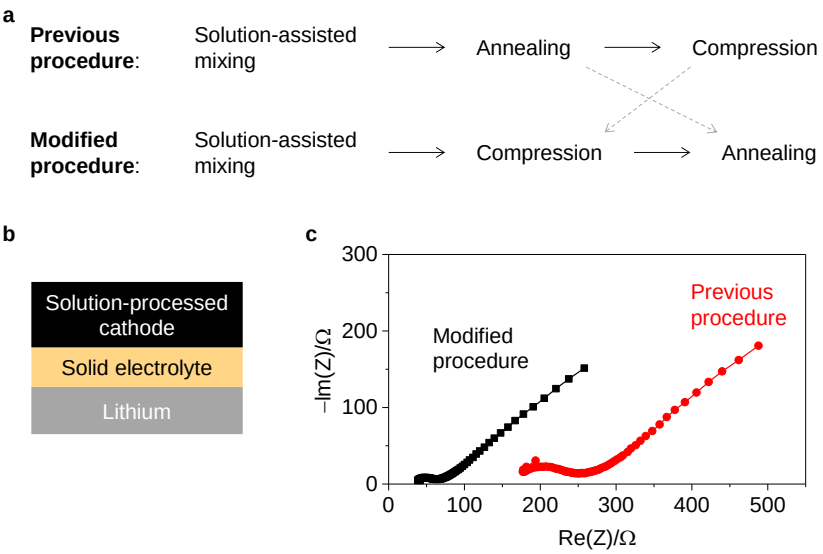

Figure 10. Fabrication and preliminary electrochemical measurement of a solid-state lithium-organic cell with a solution-processed cathode. a, Contrasting a previously reported cathode preparation procedure with a modified one. b, representative structure of the cells used for electrochemical measurements. c, Nyquist plots of cells fabricated with cathodes processed using a previously reported and a modified procedure.

Our modified procedure switches the sequence of annealing and compression, thus utilizing the low-temperature mechanical property such as the lowered moduli. Cells with the typical composite cathode/solid electrolyte/lithium trilayer structure were fabricated with the cathodes prepared with the two procedures (Fig. 10b). Electrochemical impedance spectroscopy at open circuit reveals notably lower resistance for the cell fabricated with the cathode prepared with the modified procedure, an indiccator of more efficient ion and/or electron conduction within the cathode. This is in line with our proposed cathode formation mechanism: while a hard solid electrolyte and a soft active material form an unfavorable ion transport network, a soft electrolyte precursor could solve the mechanical property mismatch and enable a higher-performance cathode.

While investigating the mehcanical properity of active materials and solid electrolyte and its impact on microsturctures, we also devote efforts towards synthesis of high-energy OIMs (Gen 3), which can now be synthesized in high purity at gram scale using chemicals and processes readily accessible to common chemistry labs. The molecular structure of Gen 3 is precisely defined and fully confirmed using standard characterization tools. The processing method for Gen 3 is similar to that for other OIMs studied in this project, though not as opptimized as that for Gen 1 at this point. Electrochemical evaluation in a liquid electrolyte versus Li allows fair comparison of the new material with the existing portfolio of OIMs. Since Gen 3 was synthesized

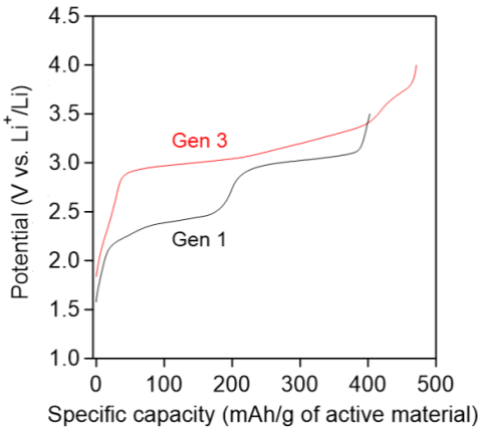

Figure 11. Charge profiles for Gen 1 and Gen 3 vs. Li in liquid electrolytes.

in the lithiated (discharged) state due to considerations discussed early in the project, we compared the charging behavior of Gen 3 with that of lithiated PTO, the benchmark OIM (Gen 1) for this project. Fig. 11 shows the potential sharply increases to two closely situated plateaus at ~2.9 and ~3.1 V before reaching a third pleateau at ~3.65 V. Overall, Gen 3 delivers an average redox potential that is ~400 mV higher than that for PTO. The first two plateaus count for a specific capacity of 200 mAh g^{-1} each while the third one counts for 75 mAh g^{-1}, leading to a total specific capacity of 475 mAh g^{-1}, again higher than the ~400 mAh g^{-1} for PTO. With notable increase in both redox potential and specific capacity, Gen 3 is expected to provide a material-level specific energy that is 30% higher than the benchmark.

The notable increase in redox potential with Gen 3 was proved to be a double-edged sword for our current recipe of solid-state Li cells. The electrochemical compatibility of OIMs and sulfide electrolytes stems from the moderate redox potentials of OIMs being within the electrochemical stability window of sulfide electrolytes, such as in the case of lithium rhodizonate and azo compounds. This project started with PTO as the benchmark OIM, the upper operation potential of which just exceeds the anodic stability limit of sulfide electrolytes. The reversibility of the PTO–sulfide electrolyte system appears good nonetheless, because sulfide electrolytes form reversible reaction products at this potential range. In the pursuit of even higher specific energy, we reported previsouly on Gen 2 and now Gen 3, both of which operate at further increased potentials. The integration of Gen 3 into sulfide electrolytes-based solid-sate cells was found to be more challenging than with Gen 1. As shown in Fig. 12, a Gen 3|LPSCl|Li cell presents an impedence of 1.1×10^5 Ohm, which is two orders of magnitude higher than that for a cell fabricated with Gen 1 through a similar procedure (8×10^2 Ohm). The spike in impedance may be attributed to the potential of Gen 3 that is well beyond the stabilty window of sulfide electrolyes. New strategies to reduce the interfacial resistance between high-energy OIMs and electrolytes will be essential for future development of OIM-based solid-state batteries. Going forward, multiple strategies appear viable to further the progress of high-energy batteries featuring OIMs. We started

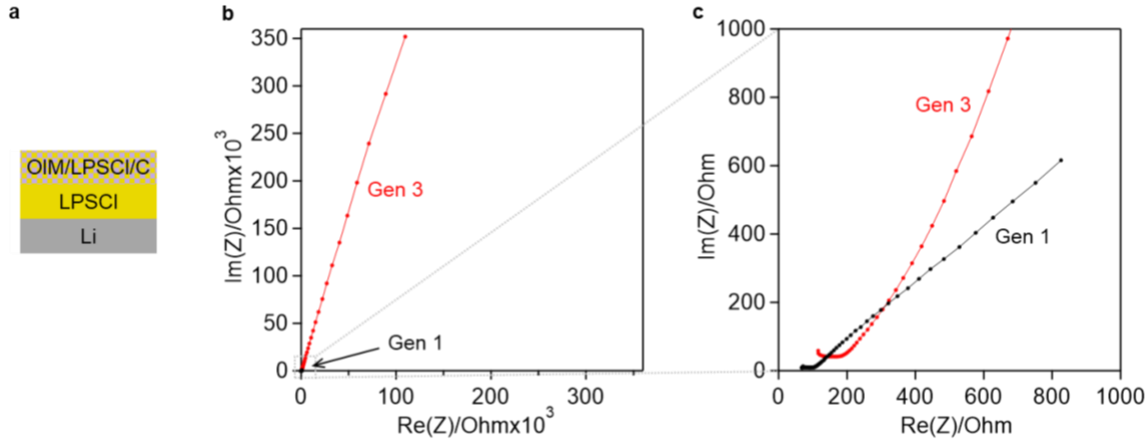

Figure 12. (a) Configuration of solid-state cells for electrochemical impedance spectroscopy (EIS) measurement. (b) EIS spectra of Gen1 and Gen3 solid-state cells at 60 °C. (c) Zoom-in on EIS spectra.

the project with sulfide electrolytes as the then-best option to be used in conjuction with OIMs. Recent years have seen the emergence of new types of solid-state electrolytes showing promising conductivity and mechanical properties. Halides and covalent organic frameworks (COFs), for example, are gaining popular due to their satisfying ionic conductivities at room temperature. Both electrolytes possess wider electrochemical stability window than that of sulfides, thus could be realistic alternatives to overcome the electrochemical/chemical incompatibility issue of sulfide electrolytes with Gen 3. Exploring OIMs with these new electrolytes could open new design space for high-performance solid-state batteries.

Publications

1. Lihong Zhao, Alae Eddine, Zhaoyang Chen, Yanliang Liang, Yan Yao*, Road map of solid-state lithium-organic batteries towards 500 Wh kg^{-1}, **ACS Energy Lett.** 2021, 6, 3287-3306.
2. Jibo Zhang, Zhaoyang Chen, Qing Ai, Tanguy Terlier, Fang Hao, Yanliang Liang, Hua Guo, Jun Lou, Yan Yao*, Microstructure engineering of solid-state composite cathode via solvent-assisted processing, **Joule,** 2021,5, 1845-1859.
3. Zhe Liu, Yunsong Li,Yanzhou Ji, Qinglin Zhang, Xingcheng Xiao, Yan Yao, Long-Qing Chen*, Yue Qi*, Dendrite-free lithium based on lesson learned from lithium and magnesium electrodeposition morphology simulations, **Cell Reports Physical Science** 2021, 2, 100294.
4. Fang Hao, Yanliang Liang, Ye Zhang, Zhaoyang Chen, Jibo Zhang, Qing Ai, Hua Guo, Zheng Fan, Jun Lou, Yan Yao*, High-Energy All-Solid-State Organic–Lithium Batteries Based on Ceramic Electrolytes, **ACS Energy Letters** 2020, 6, 201-207.
5. Yanliang Liang, Hui Dong, Doron Aurbach*, Yan Yao*, Current status and future directions of multivalent metal-ion batteries, **Nature Energy**, 2020, 5, 646-656.
6. Hui Dong, Yanliang Liang*, Oscar Tutusaus, Rana Mohtadi, Ye Zhang, Fang Hao, Yan Yao*, Directing Mg-storage chemistry in organic polymers towards high-energy Mg batteries **Joule** 2019, 3, 782-793. (Journal Cover)
7. Yang Chen, Yi Shi, Yanliang Liang, Hui Dong, Fang Hao, Audrey Wang, Yuxiang Zhu, Xiaoli Cui, and Yan Yao*, Hyperbranched PEO-Based Hyperstar Solid Polymer Electrolytes with Simultaneous Improvement of Ion Transport and Mechanical Strength, **ACS Applied Energy Materials** 2019, 2, 1608-1615.
8. Yi Shi, Yang Chen, Yanliang Liang, Justin Andrews, Hui Dong, Mengying Yuan, Wenyue Ding, Sarbajit Banerjee, Haleh Ardebili, Megan L. Robertson, Xiaoli Cui, and Yan Yao*, Chemically inert covalently networked triazole-based solid polymer electrolytes for stable all-solid-state lithium batteries, **Journal of Materials Chemistry A**, 2019, 7, 19691-19695.
9. Xiuzhen Wang, Zhenpeng Yao, Sooyeon Hwang, Ying Pan, Hui Dong, Maosen Fu, Na Li, Ke Sun, Hong Gan, Yan Yao, Alán Aspuru-Guzik, Qingyu Xu*, Dong Su*, In situ electron

microscopy investigation of sodiation of titanium disulfide nanoflakes, **ACS Nano** 2019, 13, 9421-9430.
10. Maosen Fu, Zhenpeng Yao, Xiao Ma, Hui Dong, Ke Sun, Sooyeon Hwang, Enyuan Hu, Hong Gan, Yan Yao, Eric A. Stach, Chris Wolverton, Dong Su, Expanded lithiation of titanium disulfide: Reaction kinetics of multi-step conversion reaction, **Nano Energy** 2019, 63, 103882.
11. Xiaowei Chi, Yanliang Liang, Fang Hao, Sehee Lee, Yan Yao*, Tailored organic electrode material compatible with sulfide electrolyte for stable all-solid-state sodium batteries. **Angewandte Chemie**, 2018, 130, 2660-2264. (Journal Cover)
12. Yanliang Liang, Yan Yao*, Positioning organic electrode materials in the battery landscape **Joule** 2018, 2, 1690-1709.
13. Fang Hao, Fudong Han, Yanliang Liang, Chunsheng Wang, and Yan Yao*, Architectural design and fabrication approaches for solid-state batteries. **MRS Bulletin** 2018, 43, 775-781.
14. Yanliang Liang and Yan Yao*, Advancing electrolytes towards stable organic batteries. **Green Chem**. 2017, 3, 207–212.

Acknowledgment: This material is based upon work supported by the U.S. Department of Energy's Office of Energy Efficiency and Renewable Energy (EERE), as part of the Battery 500 Consortium, Award Number DE-EE0008234.